
The formate channel FocA exports the products of mixed-acid fermentation

Wei Lü, Juan Du, Nikola J. Schwarzer, Elke Gerbig-Smentek, Oliver Einsle
& Susana L. A. Andrade

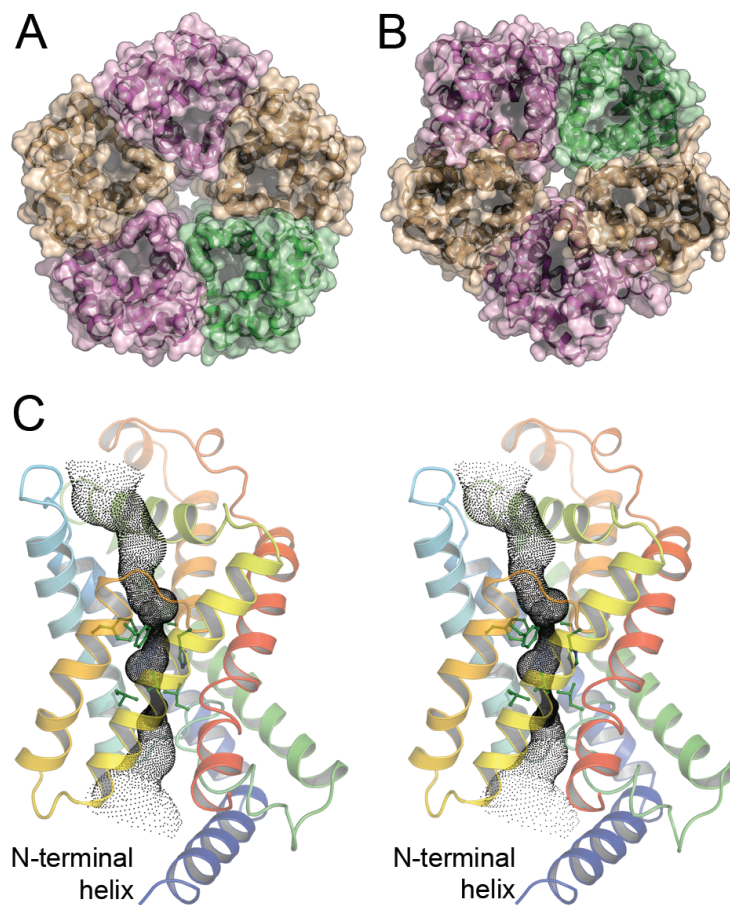


Figure S1: Three-dimensional structure of *S. typhimurium* FocA at pH 4 (PDB-ID 3Q7K). **A)** The FocA pentamer seen from the periplasmic side. Anion channels of the FNT family form stable pentamers with individual substrate channels in each protomer. **B)** Cytoplasmic view. At pH values above 5.8 the N-termini of the protomers are disordered and the protein functions as a passive channel. **C)** Stereo view of the FocA protomer (Periplasmic side above, cytoplasmic side down). The conformation of the transport channel is invariant upon pH change and contains two conserved, narrow constrictions that constitute a selectivity filter for monovalent anions.

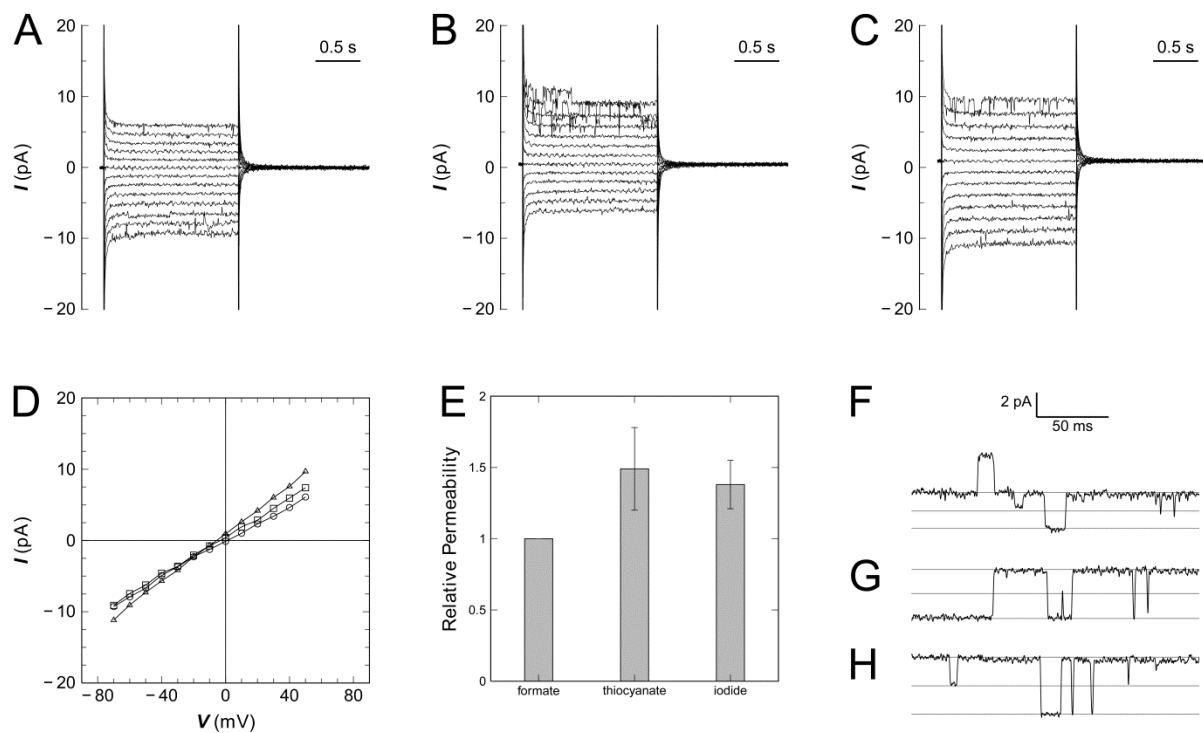


Figure S2: Inhibition of formate transport by ClC chloride channel blockers. **A)** Symmetric formate concentrations (20/20 mM) at a holding potential of 100 mV yield a linear current response as observed previously. **B)** Macroscopic currents after addition of 5 mM SCN^- to the *cis* chamber, and **C)** after equilibration of the same membrane to (5/5 mM) SCN^- and further addition of 5 mM I^- to the *cis* chamber. **D)** The I/V plot for all three recordings shows unchanged conductivity. **E)** The relative permeabilities for SCN^- and I^- are slightly higher than for HCOO^- , and single-channel recordings showed the same tendency for (20/20 mM) formate (**F**), after addition of (5/5 mM) SCN^- (**G**) and after further addition of (5/5 mM) of I^- (**H**).

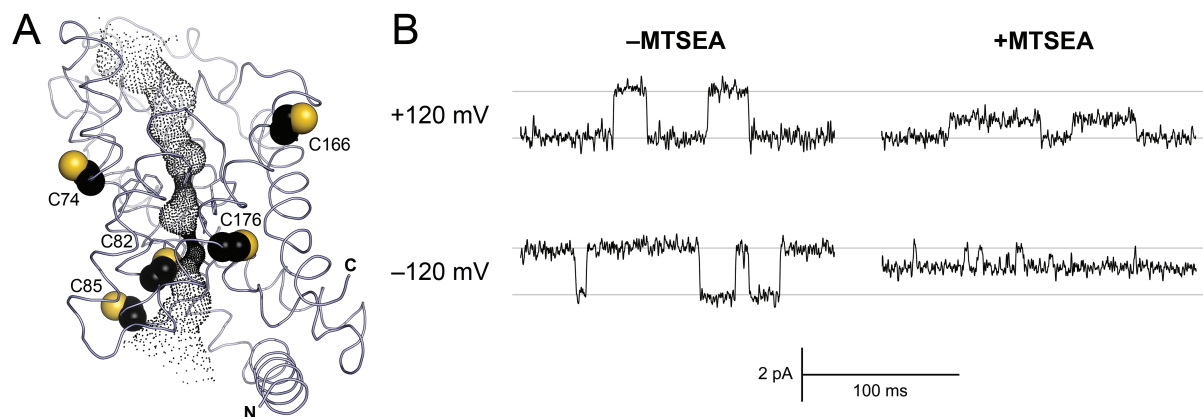


Figure S3: Specific blocking of *StFocA*. In order to confirm the identity of *FocA* after reconstitution into planar lipid bilayers, the thiol-reactive agent MTSEA (2-aminoethyl methanethiosulfonate) was added to both chambers. **A)** *StFocA* contains five cysteine residues, three of which (C82, C85, C176) are in close proximity to the transport channel. **B)** Single-channel currents change direction upon reversal of potential, and they show a marked decrease 3 min after adding MTSEA to both chambers.

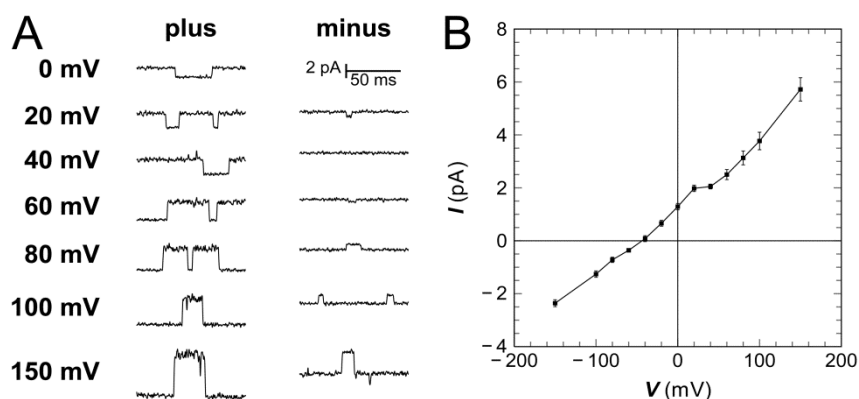


Figure S4: Single channel currents for (20/100 mM) of formate at different potentials. **A)** Individual recordings show the expected increase of current with increasing membrane potential. **B)** Averaged currents obtained from single-channel recordings yield a current/voltage diagram that reflects the correct reversal potential for formate.

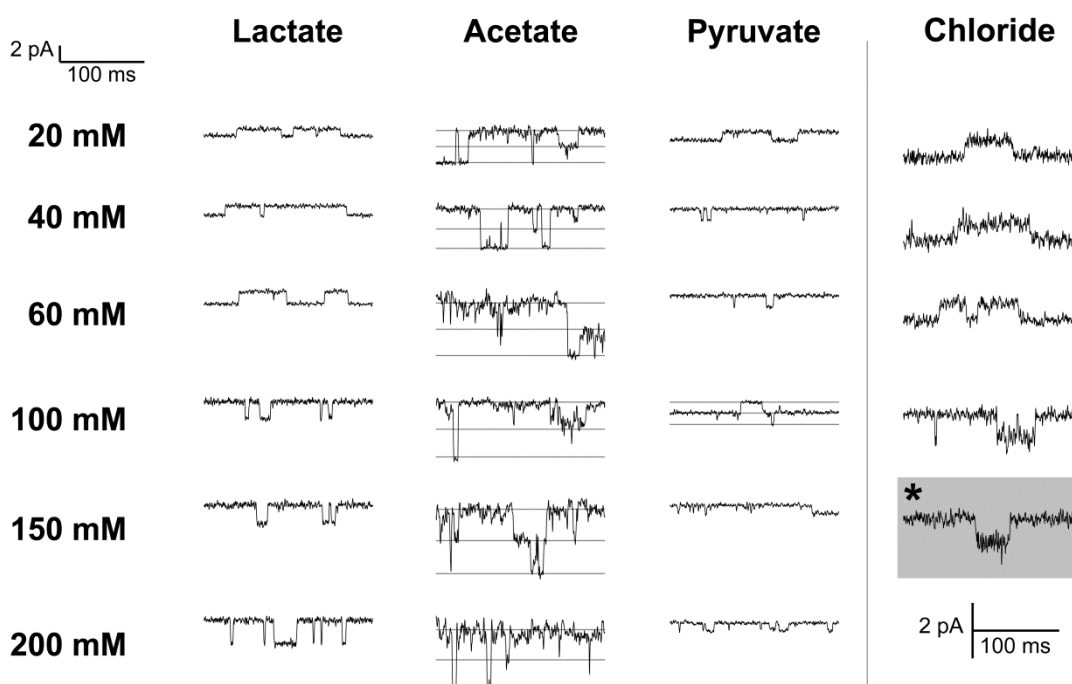


Figure S5: Single-channel currents for other permeating ions. For the three relevant ionic species in mixed-acid fermentation, lactate, acetate and pyruvate, single-channel signals were obtained that increased with concentration and were the basis for the plots shown in Fig. 3B. Single-channel currents for chloride were significantly lower (different scale), as reflected in a reduced conductance (Fig. 3B). The bottom trace for chloride (*) was recorded for (100/100 mM) NaCl in the presence of (5/5 mM) KSCN, to show that the CIC channel blocker SCN^- has no effect on chloride transport by FocA.